Proceedings of Symposium on DNS, LES and Hybrid RANS/LES Methods
ASME Fluids Engineering Division Summer Conference
August 10-14, 2008, JackconVille, FL., USA

FEDSM2008-55107

INLET CONDITIONS FOR LES OF SWIRL FLOWS

Mohammad H. Baba-Ahmadi*
School of Engineering, Computer Science and Mathematics
University of Exeter
Exeter, UK, EX4 4QF
Email: M.H.Bab-Ahmadi@exeter.ac.uk

Gavin R. Tabor
School of Engineering, Computer Science and Mathematics
University of Exeter
Exeter, UK, EX4 4QF
Email: G.R.Tabor@exeter.ac.uk

ABSTRACT

In this paper we present a novel technique for generating swirl inlets for Large Eddy Simulation (LES). The velocity a short distance downstream of the inlet to the main domain is sampled and the flow velocity data reintroduced back into the domain inlet, creating an inlet section integrated into the main domain where turbulence can develop. Additionally, variable artificial body forces and velocity corrections are imposed in this inlet section, with feedback control to force the flow towards desired swirl, mean and turbulent profiles. The method has been applied to swirling flow in a circular pipe and in an axisymmetric sudden expansion, and for the latter case compared against experimental and literature LES data, and against similar results in the literature. The method generates excellent results, and is elegant and straightforward to implement.

NOMENCLATURE

B SGS stress tensor
$\mathbf{F}$ Body force
G Filter function.
GS Grid scale
L Length of mapping section
R_0 Radius of nozzle
R_{des} Desired Reynolds stress
R_{ii} Primary components of Reynolds stress tensor
S Strain rate tensor
SGS Sub-grid scale
$\overline{\mathbf{v}}$ Grid scale velocity vector
$\mathbf{v}$ Velocity vector
V_b Bulk velocity
$\mathbf{v}_{des}$ Desired mean flow profile
$\mathbf{v}'$ Sub-grid scale velocity vector
v_z, v_θ Axial,tangential components of velocity
α Feedback factor
Δ Characteristic length
ν Static viscosity
ρ Density

INTRODUCTION

Swirl injectors have been widely adopted in combustion systems such as gas-turbine engine combustors to stabilise the flame for efficient and clean combustion. Breakdown of the incoming swirl vortex in the central toroidal recirculation zone creates high shear rates and strong turbulence intensities which act as a flame stabilisation mechanism. In addition, the swirl also produces high rates of entrainment and fast mixing. Modelling of these processes however is extremely complicated. In particular, swirling flows are difficult to model with Reynolds Averaged Navier Stokes (RANS) methods due to the effect of the mean flow streamline curvature [1], so this is one example where LES methods have come to the fore. However there are still numerous technical issues to be overcome in implementing LES as a technique [2]. In particular, the provision of adequate boundary conditions, and for the case of swirl injection this means particularly inlet conditions, is one very significant hurdle to be over-

*Address all correspondence to this author.

come, and this is the subject of the current paper. Implementing inlet conditions for LES is siginificantly more challenging than is the case for RANS models; the inlet flow has to include the grid scale (GS) turbulence, and so has to include a stochastically fluctuating component which satisfies a range of conditions (such as the correct temporal and spatial correlation). Thus the topic of this paper is of great importance for the adoption of LES in this area.

Two approaches to creating inlet conditions for swirling flow have been applied in the literature. The simplest approach is to create a mean flow profile by determining the axial and tangential mean flow components, either from previous computational work (using RANS), or from experiment, or from theory, and impose a specified level of fluctuation on top of this, usually as Gaussian white noise. Examples of this approach include [3, 4]. However such approaches suffer problems related to the non-physical nature of the 'turbulence' introduced at the inlet, leading to incorrect prediction of turbulent kinetic energy and energy spectra downstream of the inlet [5]. The alternative approach is via a turbulence library database. Typically this involves running a precursor simulation on a simpler geometry, eg. a cyclic channel, to create fully-developed turbulence; successive time steps of this simulation are then saved and replayed into the inlet of the main simulation. Various variants of the technique have been tried, for example running the precursor simulation in parallel with the main simulation (thus obviating the need to store a limited database of information [6]), and scaling the data using the Reynolds stress (to adjust an existing database to another Reynolds number, e.g. [7]). In the context of swirling flows, most versions of this technique make use of a method developed by Pierce and Moin [8] for generating swirl within a cyclic channel by imposing a constant tangential body force on the flow. Having computed a library of turbulent swirling flow in this way, either as a saved precursor database or 'on the fly' in parallel with the main calculation, the flow conditions from the secondary calculation can be fed into the main computation [9, 10]. As an example of this, Wang and Bai [5] use Pierce and Moin's method to create a 10,000 timestep library for lookup which is then cycled through as appropriate. The library however does not meet the specifications for the required flow, and so the data is rescaled to meet the desired statistical properties (specified mean and variance of velocity). However this rescaling does cause problems; the level of turbulent kinetic energy is seen to decrease downstream of the inlet, which the authors attribute to the unphysical turbulence at the inlet adapting to become true turbulent flow further downstream. Schlüter *et al.* [11] also implement and compare various inlet conditions for swirl, specifically a laminar inflow (no fluctuations), inflow with random fluctuations, and various precomputation methods. As before, the laminar and random fluctuation techniques produce poor results, whilst the various library lookup techniques perform much better.

In the current work we present a novel technique for generating an inlet for generating swirl flow for LES by applying a body force and remapping within the main computational domain. Hence; a region of the main computational domain is designated as the inlet region; at the end of this region the flow conditions are sampled and fed back into the start of the computational domain. At this level, this approach has been demonstrated to work well in the past [12, 13]. In addition axial and tangential body forces are introduced within the inlet section together with velocity correction terms in this region; feedback control is used to modify these terms in order to drive the flow towards the desired velocity profiles (including swirl) and turbulence profiles. Our method thus differs from existing published work for swirl inlets in two important details, a. the turbulence development region is integrated into the main domain rather than having to be run as a separate calculation, and b. the body force is varying rather than fixed, and is controlled so as to develop very precisely the correct mean and turbulence flow conditions. We also incorporate a correction method to improve the turbulence statistics for the flow; this has been applied before in the literature to generate libraries for lookup [7]; however this is the first time that this method has been applied directly to the main domain in this manner, and applied to generate a swirling flow. As a preliminary test case we have applied the method to swirling flow in a cylindrical pipe. Following on from this we apply it to the case of incompressible flow over a cylindrical sudden expansion. This is a canonical test case for swirling flows, where a jet of fluid with or without swirl enters a much larger cylindrical geometry, and for which there is a significant ammount of experimental and computational data to compare with. In essence it recreates many of the features of gas turbine injectors and dump combustors, as well as jets entering larger domains.

THEORY

LES and numerical implementation

LES is based on a spatial averaging in the form of a convolution with a spatial filter G, separating the flow into grid scale (GS) and sub-grid scale (SGS) components $\mathbf{v} = \overline{\mathbf{v}} + \overline{\mathbf{v}'}$, where $\overline{\mathbf{v}} = G * \mathbf{v} = \int_D G(\zeta, \Delta)\mathbf{v}(\zeta, t)d^3\zeta$, Δ is a characteristic scale of G, referred to as the filter width, and D is the computational domain. Conventionally we assume that the filter width is the same as the cell size Δx, hence the labels Grid Scale and Sub-Grid Scale. In this case the averaged, or filtered Navier-Stokes equations take the form

$$\begin{aligned} &\nabla.\overline{\mathbf{v}} = 0, \\ &\partial_t\overline{\mathbf{v}} + \nabla.(\overline{\mathbf{v}}_{\otimes}\overline{\mathbf{v}}) = \nabla.(\overline{\mathbf{S}} - \mathbf{B}) + \overline{\mathbf{F}}, \end{aligned} \tag{1}$$

given that $[G*, \nabla]\mathbf{v} = \mathbf{0}$: $\mathbf{v}$ is the velocity field, ν the molecular viscosity, $\mathbf{S} = -p\mathbf{I} + 2\nu\mathbf{D}$ with p the specific pressure, and $\mathbf{D} =$

$\frac{1}{2}(\nabla\mathbf{v}+\nabla\mathbf{v}^T)$. The convolution process generates an additional term, the SGS stress tensor :

$$\mathbf{B} = \overline{\mathbf{v}\otimes\mathbf{v}} - \overline{\mathbf{v}}\otimes\overline{\mathbf{v}} = \mathbf{L}+\mathbf{C}+\mathbf{R}, \tag{2}$$

where **L** is the Leonard stress, **C** the cross stress and **R** the Reynolds stress tensor (e.g. [14]). Different modelling of these terms generates the different turbulence models; here we use the dynamic one-equation model [15]. $\overline{\mathbf{F}}$ represents an artificial body force term that will be discussed below.

The filtered Navier-Stokes equations, (1) together with (2), are solved using the CFD code library OpenFOAM. This is a C++ code library of classes for writing CFD codes, which includes a well-tested and validated LES capability [14, 16–18]. Equations (1) are discretized using the finite volume method. For interpolation onto the faces to generate the fluxes we use centred second order interpolation and NVD-derived interpolation (gamma scheme, see [19]), whilst time integration is carried out by the Crank-Nicholson scheme, which is also 2nd order. The full equation set is solved sequentially using the resulting PISO algorithm [20]. SGS modelling is provided by the dynamic 1-equation model, in which a transport equation is provided for the sub-grid turbulent kinetic energy *k*, and the resulting model coefficients can be determined by introducing a second, grid-scale level of filtering [15]. The one-equation approach may allow for coarser grids than can be used for a comparable problem with a zero-equation model because some sub-grid information is available for the formulation of sub-grid scale models. All of this has been implemented in OpenFOAM previously and extensively validated [14].

Inlet Conditions.

Included in the governing equations to be solved is a term $\overline{\mathbf{F}}$, which will be used to drive the flow towards the desired swirl. This term is non-zero within the inlet section of the mesh, where it takes the value

$$\overline{\mathbf{F}} = \frac{V_b}{L}\left[\alpha(\mathbf{v}_{des}-\langle\overline{\mathbf{v}}\rangle)+(\mathbf{v}_{des}-\overline{\mathbf{v}})\right], \tag{3}$$

Here, $\mathbf{v}_{des}$ is the target mean flow profile and $\overline{\mathbf{v}}$ the instantaneous GS velocity. $\langle\overline{\mathbf{v}}\rangle$ is the time average of the GS velocity, evaluated by taking a running average on the GS velocity. Also V_b and L are the desired bulk velocity and the length of the forcing region respectively. L was varied by trial and error to get the best results from the simulation; the value used here of $z/R = 4$ corresponds to around 1500 wall units which should be adequate for turbulence to develop fully.

In Eqn (3), the first term in the bracket *i.e.* $\alpha(\mathbf{v}_{des}-\langle\overline{\mathbf{v}}\rangle)$ provides feedback control on the mean flow, with α setting the magnitude of the feedback. The second term $(\mathbf{v}_{des}-\overline{\mathbf{v}})$ provides some control over the magnitude of instantaneous fluctuations in the velocity (i.e. the GS turbulence). However, early in the simulation $\mathbf{v}_{des}-\langle\overline{\mathbf{v}}\rangle$ is large, with potentially unfortunate consequences. Thus at the start of the simulation, the value $\alpha = 0$ is chosen. As the simulation progresses $\mathbf{v}_{des}-\langle\overline{\mathbf{v}}\rangle$ decreases towards zero, so the value of α is ramped to a maximum value determined so that $|\mathbf{v}_{des}-\langle\overline{\mathbf{v}}\rangle|/V_b < 0.0001$. If α was allowed to increase without limit, the force contribution from this term would eventually come to dominate the equation for no physical reason and the simulation would fail.

This control mechanism drives the mean flow towards the desired target $\mathbf{v}_{des}$ – in this case the experimentally - determined mean flow profiles in the axial (and for the swirling flow) tangential directions. We are also interested in generating the correct turbulence profiles, and in order to achieve this a second level of feedback control is provided by correcting the velocity components within the inlet section using the relation

$$\overline{\mathbf{v}}^* = \mathbf{v}_{des} + (\overline{\mathbf{v}}-\langle\overline{\mathbf{v}}\rangle)\times\left(\frac{(R_{des})_{ii}}{R_{ii}}\right)^{1/2}, \tag{4}$$

where R_{des} is the desired Reynolds stress and R is the calculated GS Reynolds stress in the mapping section, evaluated by means of a running average. Note that Einstein summation convention is not used; we scale the fluctuations by differing ammounts in each direction. The SGS contribution to the calculated Reynolds stress could have been included here, but since we are using an eddy viscosity SGS model this would have introduced further assumptions about the isotropy of the turbulence at small length scales. The velocity $\overline{\mathbf{v}}$ is replaced by the updated velocity $\overline{\mathbf{v}}^*$ in each cell in the inlet section. Because of the fluctuations, the term $(\overline{\mathbf{v}}-\langle\overline{\mathbf{v}}\rangle)$ is never exactly zero, and so the term $\left(\frac{(R_{des})_{ii}}{R_{jj}}\right)^{1/2}$ drives the turbulent fluctuations to provide the target root mean square mean velocity components and in turn the target axial components of the Reynolds stress. This relation was first implemented in [7] to generate a database for lookup based on an *a priori* RANS calculation; here it is applied directly to control the flow. The case being simulated [21] provides experimental measurement of the flow conditions upstream of the inlet, and these were used as the target profiles for the mean and fluctuating velocity components.

Test Cases

Results from two test cases are presented here; the first being that of swirling flow in a cylindrical pipe of length $10D$, where the pipe diameter $D = 2$ m. The mesh resolution is 448 cells covering the cross section and 30 cells per meter of length. The level of swirl in the flow is expressed in terms of the swirl num-

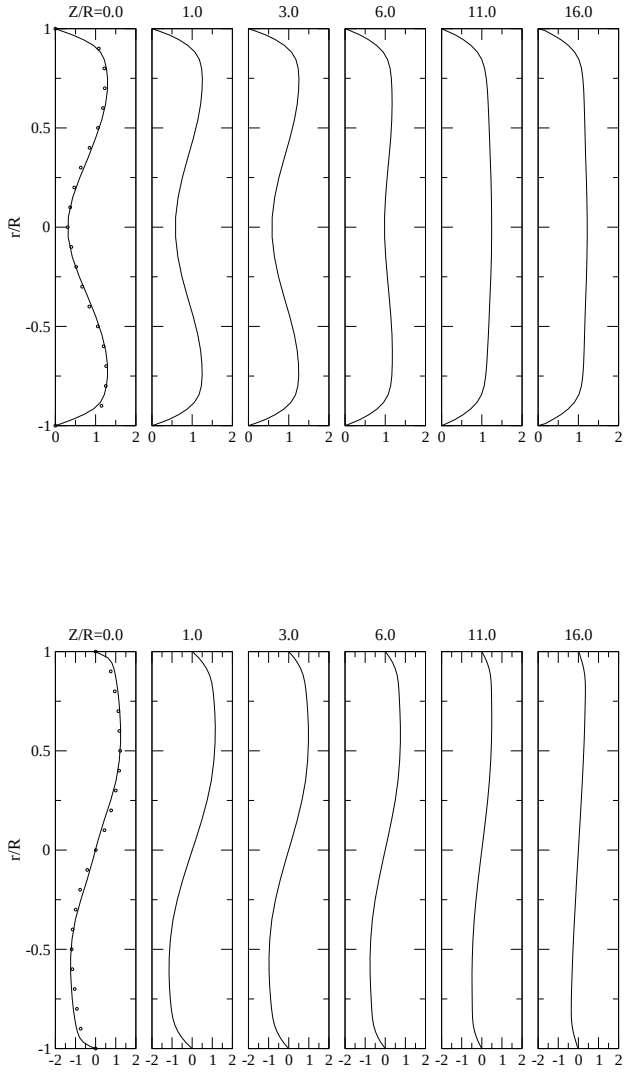

Figure 1. AXIAL AND TANGENTIAL MEAN VELOCITY PROFILES AT DIFFERENT DISTANCES FROM THE INLET OF THE MAIN DOMAIN. SOLID LINES: LES DATA, CIRCLES: SHORT PIPE FLOW.

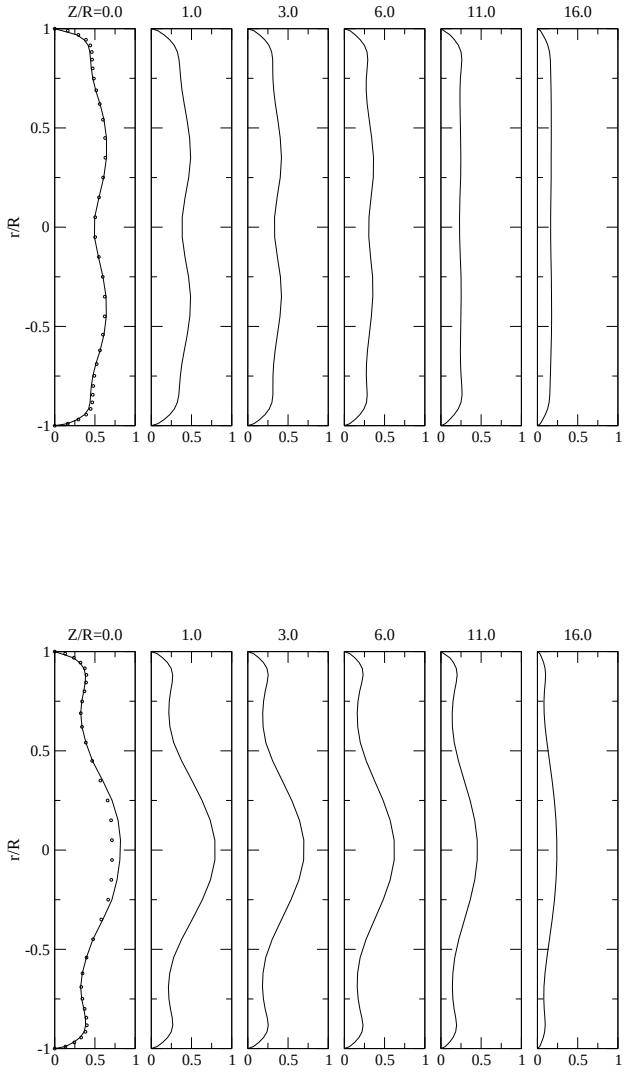

Figure 2. $v'_{z,rms}$ and $v'_{\theta,rms}$ AT DIFFERENT DISTANCES FROM THE INLET OF THE MAIN DOMAIN. SOLID LINES: LES DATA, CIRCLES: SHORT PIPE FLOW.

ber, which is the ratio of angular momentum flux in the axial direction to the axial momentum flux in the axial direction, i.e.

$$S = \frac{1}{R_0} \frac{\int_0^{R_0} r^2 \langle v_z \rangle \langle v_\theta \rangle dr}{\int_0^{R_0} r \langle v_z \rangle^2 dr} \tag{5}$$

where $\langle v_z \rangle$ is the axial velocity component, $\langle v_\theta \rangle$ is the azimuthal velocity component, and R_0 is the radius of the nozzle. For the pipe flow, the level of swirl introduced corresponded to a swirl number of 0.6, with target axial, tangential velocity profiles and r.m.s. velocity profiles provided from experimental data [21]. This case is run for a swirl number $S = 0.6$ at $\mathcal{R}e = 30,000$. This case was run for 4000 s with a timestep of $\Delta t = 0.05$ s, equivalent to 60 complete transits of the flow through the domain.

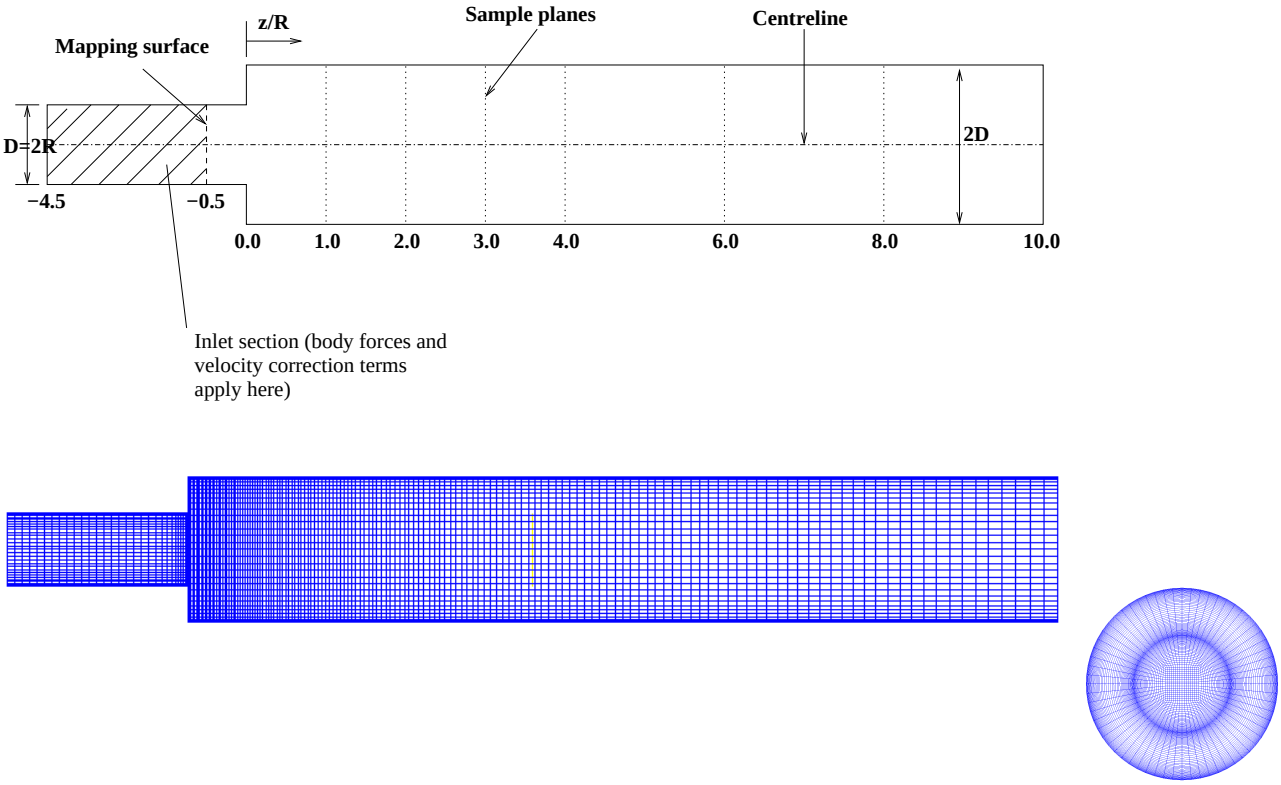

Figure 3. GEOMETRY FOR SWIRLING JET FLOW IN SUDDEN EXPANSION. TOP FIGURE: GEOMETRY AND LOCATION OF MAPPING SURFACE AND SAMPLE PLANES. MIDDLE FIGURE: CROSS SECTION THROUGH THE MESH. BOTTOM FIGURE: END VIEW OF THE MESH.

The second geometry used corresponds to the experiments of Dellenback *et al.* [21], who undertook measurements in a turbulent swirling flow through an abrupt axisymmetric expansion and examined the influence of the swirl number. We present results for a computed flow with a swirl number $S = 0.6$ at $\mathcal{R}e = 30,000$. Swirl flows at high swirl numbers $(S > 0.25)$ create central recirculation zones [7], and, as a result of that, flows with high shear are created which have a high level of turbulence production. The mesh used for this computation consists of a $248 \times 76 \times 76$ cylindrical block mesh using approximately 1.5 million cells for computational domain, with the smallest cells next to the edge of the jet. The cell size near the wall upstream of the expansion is approximately $y^+ = 16$, which means that the boundary layer is still under-resolved. The finer mesh required a shorter timestep of $\Delta t = 0.0125$ s. This case was run for 1500 s, equivalent to 30 complete transits of the flow through the domain.

In addition to the experimental data, this test case has been used for LES simulation before, in particular by Schlüter *et al.* [7]. They used an LES flow solver developed at the Centre for Turbulence Research [8].This flow solver solves the filtered momentum equations with a low Mach number assumption on an axisymmetric structured mesh with a second order finite volume scheme on a staggered grid. Subgrid stresses are modelled with an eddy viscosity approach coupled to the dynamic procedure. For inlet conditions they used a precomputed library modified to account for the unsteadiness of the interface flow statistics. Numerical results are available for the swirl case and have been included in the comparison.

RESULTS

Pipe flow case

Results for the mean profiles of $\langle u_z \rangle, \langle u_\theta \rangle, \tau_{zz}$ and $\tau_{\theta\theta}$ at different distances from the inlet are presented in the figures 1-2. The inlet target profiles were generated by running a subsidiary calculation on a short cyclic pipe under the same conditions as for the case of Dellenback [21]; a swirl number $S = 0.6$ at $\mathcal{R}e = 30,000$. This data was averaged and used as the target profile. We do not have data to compare with the calculated results, so the desired profile is reproduced on the graphs (circles) at the end of the recirculation region of the domain ($z/R = 0$). Agreement between computed and target profiles at this position is very close. The profiles evolve downstream as the swirl in the flow decays, as should be expected. Figure 4.A. plots enstrophy on a plane through the domain. The decay of the swirl vortex is very apparent in this plot. There is some slight difference in

the near-wall region of the flow in the mapped section versus the downstream section of the domain; the bulk rotation of the fluid in the mapped section is being maintained by the body forces, whilst these are absent further downstream so the boundary layer can expand into the flow. There is no sign of discontinuity in the flow going from the mapped section to the main domain, nor signs of significant periodicity downstream of the mapped section.

Sudden expansion case

Figures 5-6 show the results for this computation. The results (full lines) are compared with experimental results (dotted lines) and Schlüter results *et al.* [7] results (dot-dash lines). In this case, despite some small discrepancies especially near the edge of the expansion, the results agree very well with experimental data near the outlet, in contrast to the previous case ($S = 0.0$). This can be explained by the fact that the level of internal turbulence production due to the breakdown of the swirl in this type of flow is rather high behind the expansion; thus the relative effect of turbulence entering the domain at the inlet is much less. The origin of the inner recirculation zone in highly swirling flows is fixed at the location of the expansion, which means that the zones of turbulence production – the shear layers created by the recirculating fluid and the issuing jet – are well determined and independent of the inflow conditions. The turbulence level is then almost entirely defined by the turbulence production behind the step, which makes the flow almost independent of the inlet turbulence intensity. This case shows that situations exist where the inlet turbulence plays a minor role, even when complex flow configurations are considered. In this special case, the high level of turbulence production inside the LES domain is dominant and its location and level are not determined by the inlet turbulence conditions. However generating the correct mean (swirling) flow is still crucial in producing the correct results, and as can be seen from Fig. 5, our method is performing rather well for this.

Analysis

The two cases being computed demonstrate significant features of importance in swirling flows. The pipe flow case was used as a trial to develop the methodology being used, rather than matching specific experimental or computational data. The most important aspects of the computation are its demonstration that the flow form is uniform across the mapping plane and does not demonstrate unphysical behaviour downstream of the mapped section of the domain. In particular there is little sign of excessive periodic behaviour downstream of the mapped section. Periodicity is an important problem with library-lookup methods, due to the finite length of the database. Some degree of periodicity is to be expected with our method, but the flow is evolved each time it recirculates through the inlet section, so the periodicity is less than might be thought.

The sudden expansion test case was set up to reproduce specific experimental data, in order to provide a more complete validation of the method. The mean flow in the body of the domain is generally well reproduced by our LES. Some discrepancies are seen directly downstream of the inlet for the axial velocity (figure 5), but our method performs at least as well as the comparison LES data from Schlüter *et al.* The r.m.s. velocity profiles are also well predicted, except for a short distance downstream of the expansion in the case of the no-swirl test case. In general, for all properties, our results are comparable with or better than the comparison LES data. In particular no additional length of inlet is required for the turbulent fluctuations to develop in any way, and there is no significant impact on the flow behaviour in the inlet section due to the additional modelling in this region. As observed elsewhere [11], zero and low-swirl cases are strongly sensitive to fluctuations in the inlet velocity, and inlet methods which do not account for this behaviour (e.g. laminar or white noise inlets) fail to perform at all well. High swirl cases are more dominated by the breakdown of the swirl vortex to turbulence and so are less sensitive to turbulence at the inlet, and in fact laminar and white-noise inlet conditions can be shown to produce reasonable results, at least for the mean flow profiles [11]. However it is still necessary to generate the mean swirl flow, which our method does efficiently and completely. A low-swirl case (e.g. $S = 0.3$) would show our method in the best light, since this would require swirl inlet but still be sensitive to inlet turbulence; however much less comparison data is available for this case. The behaviour of our method is still convincing, and we conclude that our method is a significant improvement over laminar or white-noise synthesis inlets for this case.

Compared with library lookup, our method performs well, but the differences are more nuanced. Our results for the sudden expansion swirl case are at least as good as those of Schlüter *et al.* [11], and are better in places. Part of this may be because we are able to base the target flow directly on the experimentally determined profiles, although if this data were not available there would be no reason why we could not develop $\mathbf{v}_{des}$ analytically for a desired swirl number. Additionally, our method is simpler to apply. For a library lookup method, a suitable auxiliary calculation has to be set up and simulated; the data must be stored for use, and recycling this data can introduce unwanted periodic behaviour into the flow, and restrict the time span used for generating flow statistics in the main domain. Running the auxiliary computation at the same time as the main calculation obviates these problem, but introduces its own programming problems. Additionally, if the flow conditions change (eg. a different Reynolds number) then the library must be recomputed or rescaled; the latter can be shown to introduce additional problems into the simulation [5]. Integrating the auxiliary computation into the main domain in this manner, on the other hand, is much more elegant and easier to manage, and generates extremely good mean and turbulent flow results. The relative com-

A.

B.

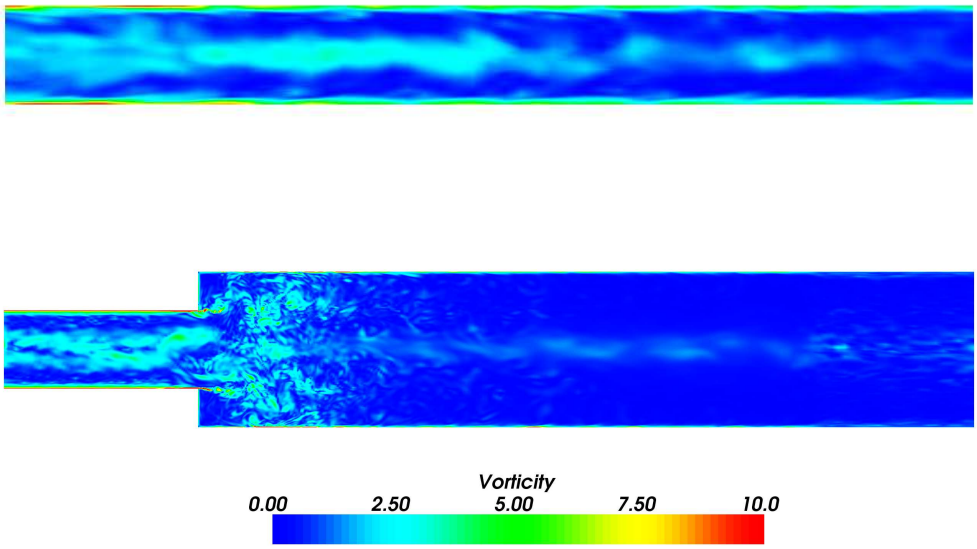

Figure 4. VORTICITY ON MIDPLANE OF GEOMETRY. A. SWIRLING PIPE FLOW, B. SWIRLING JET FLOW

putational costs of the different methods may vary according to the exact problem being simulated. If the main domain needs to be extended to provide an inlet section for our mapping method, then this will impose an increased computational requirement on the main calculation, which would be comparable with the cost of running an auxilliary calculation. Indeed, if the auxilliary calculation can be reduced in scale, eg. by storing a short dataset or using a longer timestep, then this might reduce the computational cost for the library method. However these steps impose problems of their own (for instance interpolation between saved timesteps if a longer timestep is used for the auxilliary calculation). For our mapping case presented here, the inlet cells represent approximately 5% of the total, so the computational costs associated with these additional cells are relatively minor. Additionally, the inclusion of the additional and corrective terms into the NSE for the inlet section does seem to have little negative impact on the flow in this region, so it may be possible for the mapping to take place on a section of mesh which is part of the desired physical domain, not simply an additional extension to the computational domain.

CONCLUSION

In this paper we have presented a novel technique for generating swirl inlets for LES. The technique involves introducing an artificial body force and velocity correction terms into the early part of the computational domain (designated as the inlet section) with remapping of the velocity from the end of the inlet section back to the domain inlet. Control algorithms are used to vary the body force and velocity correction in order to generate desired swirl, mean velocity, and Reynolds stress profiles. The method has been applied to pipe flow and flow in an axisymmetric sudden expansion, with swirl at the inlet, and compared against experimental and literature LES data, and against similar results in the literature. The method generates excellent results for this case, in particular matching mean and fluctuating components of the velocity very precisely. We find no negative impact on the turbulence properties as evidenced from the enstrophy. Finally, the method is elegant and straightforward to implement.

ACKNOWLEDGMENT

GRT, MHB-A acknowledge the support of the EPSRC through grant GR/R27495/01. We would like to thank Dr Swaminathan for computer time to perform the computations, and Prof. Schlüter and Prof. Dellenback for access to their LES

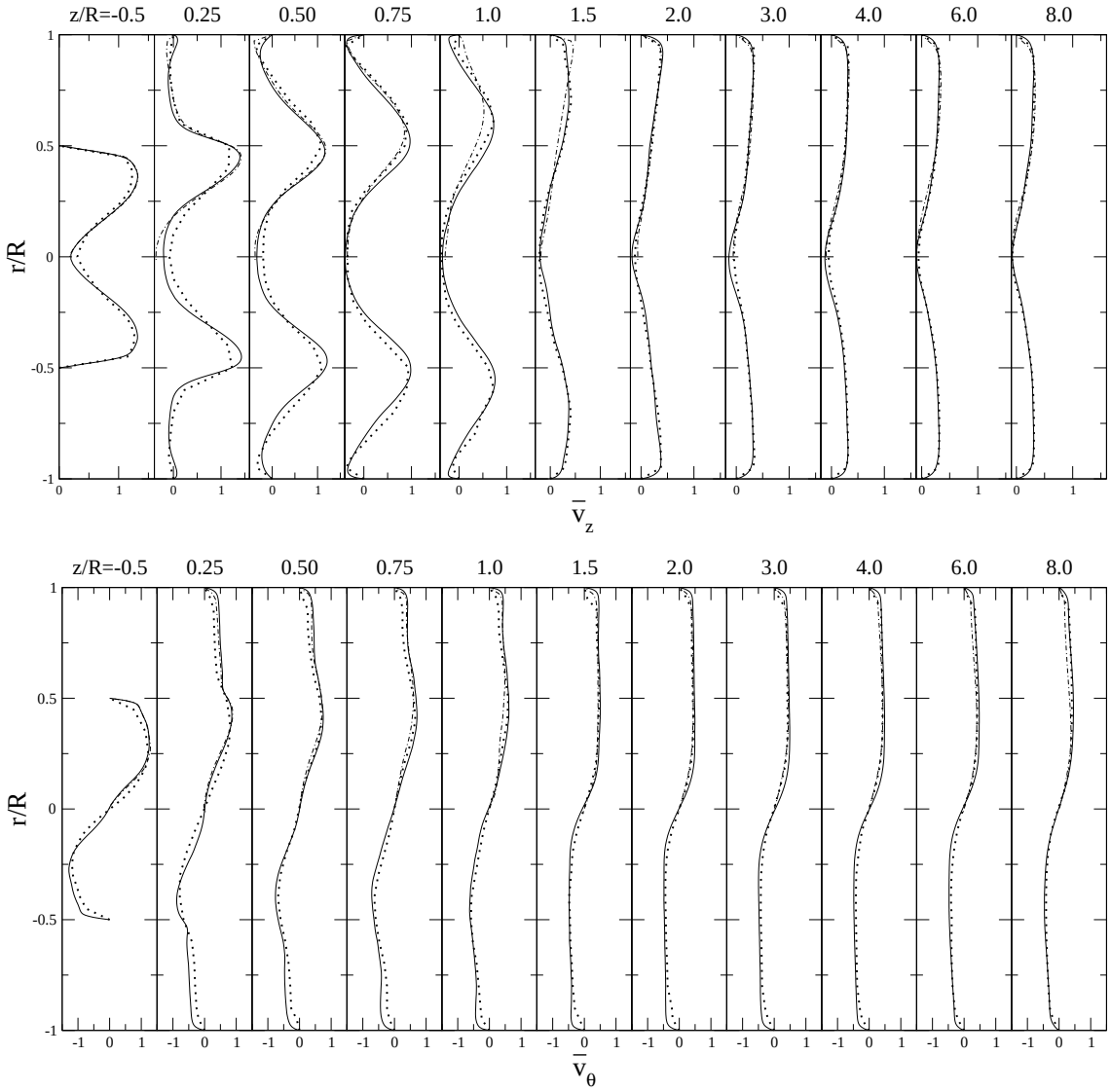

Figure 5. AXIAL AND TANGENTIAL MEAN VELOCITY PROFILES AT DIFFERENT DISTANCES FROM THE INLET OF THE MAIN DOMAIN. DOTTED LINES: EXPERIMENTAL DATA, SOLID LINES: LES DATA, dOT-DASH LINES: SCHLÜTER *ET AL*. DATA.

and experimental results, respectively.

REFERENCES

[1] Jakirli, S., Hanjali, K., and Tropea, C., 2002. "Modelling rotating and swirling turbulent flows: a perpetual challenge". *AIAA J.*, **40**(10), pp. 1984–1996.

[2] Pope, S. B., 2004. "Ten questions concerning the large-eddy simulation of turbulent flows". *New Journal of Physics*, **6**(35), DOI:10.1088/1367-2630/6/1/035.

[3] Huang, Y., and Yang, V., 2005. "Effect of swirl on combustion dynmics in a lean-premixed swirl-stabilized combustor". *Proceedings of the Combustion Institute*, **30**, pp. 1775–1782.

[4] Wang, S., Yang, V., Hsiao, G., Hsieh, S. Y., and Mongia, H. C., 2007. "Large-eddy simulations of gas-turbine swirl injector flow dynamics". *Journal of Fluid Mechanics*, **583**, pp. 99–122.

[5] Wang, P., and Bai, X., 2005. "Large eddy simulations of turbulent swirling flows in a dump combustor: a sensitivity study". *International Journal of Numerical Methods in Fluids*, **47**, pp. 99–120.

[6] Lund, T. S., Wu, X., and Squires, K. D., 1998. "Generation of Turbulent Inflow Data for Spatially-Developing Bound-

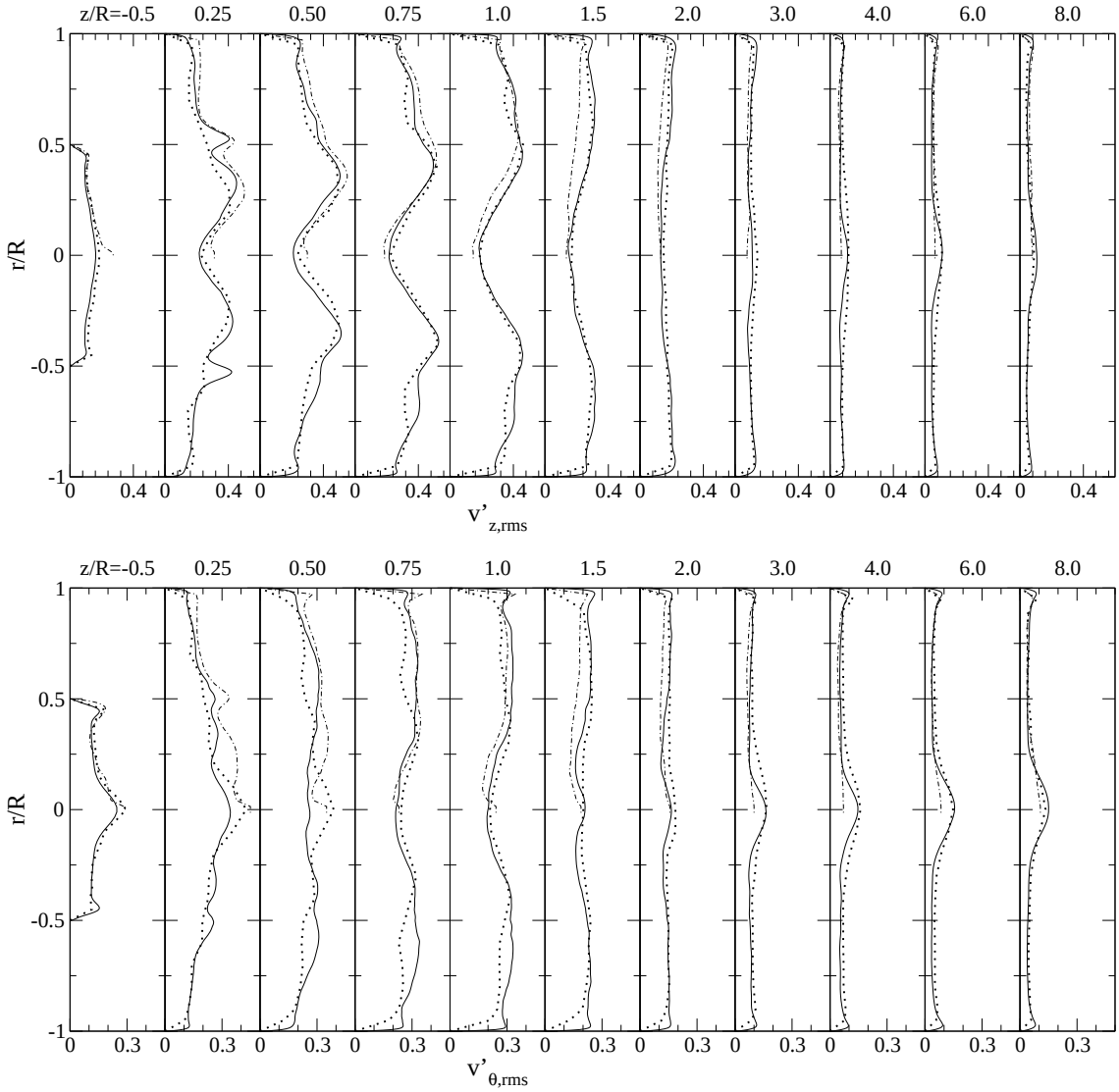

Figure 6. $v'_{z,rms}$ and $v'_{\theta,rms}$ AT DIFFERENT DISTANCES FROM THE INLET OF THE MAIN DOMAIN. DOTTED LINES: EXPERIMENTAL DATA, SOLID LINES: LES DATA, dOT-DASH LINES: SCHLÜTER *ET AL.* DATA.

ary Layer Simulations". *Journal of Computational Physics*, **140**, pp. 233–258.

[7] Schluter, J. U., Pitsch, H., and Moin, P., 2004. "Large Eddy Simulation Inflow Conditions for Coupling with Reynolds-Averaged Flow Solvers". *AIAA.J.*, **42**(3), March, pp. 478–484.

[8] Pierce, C. D., and Moin, P., 1998. "Large Eddy Simulation of a Confined Coaxial Jet with Swirl and Heat Release". *AIAA.J.*, **98**, p. 2892.

[9] Wang, P., Bai, X. S., Wessman, M., and Klingmann, J., 2004. "Large eddy simulation and experimental studies of a confined turbulent swirling flow". *Physics of Fluids*, **16**, pp. 3306–3324.

[10] Garcia-Villalba, M., and Frohlich, J., 2006. "Les of a free annular swirling jet – dependence of coherent structures on a pilot jet and the level of swirl". *International Journal of Heat and Fluid Flow*, **27**(5), pp. 911–923.

[11] Schluter, J. U., Pitsch, H., and Moin, P., 2003. "Boundary Conditions for LES in Coupled Simulations". *Tech. Rep. AIAA-2003-0069*(41st Aerospace Sciences Meeting), Jan 6-9.

[12] Tabor, G., Baba-Ahmadi, M. H., de Villiers, E., and Weller, H. G., 2004. "Construction of Inlet Conditions for LES of Turbulent Channel Flow". *Proceedings of the ECCOMAS*

Congress, Jyvaskyla, Finland.

[13] de Villiers, E., 2006. "The Potential for Large Eddy simulation for the modelling of wall bounded flows". PhD Thesis, Imperial College, London, UK.

[14] Fureby, C., Tabor, G., Weller, H. G., and Gosman, A. D., 1997. "A comparative study of sub grid scale models in homogeneous isotropic turbulence". *Physics of Fluids*, **9**(5), pp. 1416–1429.

[15] Ghosal, S., Lund, T. S., Moin, P., and Akselvoll, K., 1995. "A dynamic localization model for large eddy simulation of turbulent flows". *Journal of Fluid Mechanics*, **286**, pp. 229–255.

[16] Fureby, C., Gosman, A. D., Tabor, G., Weller, H. G., Sandham, N., and Wolfshtein, M., 1997. "Large Eddy Simulation of Turbulent Channel Flows". *Proceedings of Turbulent Shear Flows 11*, **3**, pp. 28–13.

[17] Fureby, C., Tabor, G., Weller, H., and Gosman, A. D., 1997. "Differential subgrid stress models in large eddy simulations". *Physics of Fluids*, **9**(11), pp. 3578–3580.

[18] Fureby, C., Tabor, G., Weller, H. G., and Gosman, A. D., 2000. "Large Eddy Simulation of the Flow Around a Square Prism". *AIAA.J.*, **38**(3), pp. 442–452.

[19] Jasak, H., Weller, H., and Gosman, A., 1999. "High resolution nvd differencing scheme for arbitrarily unstructured meshes". *International Jourmal of Numerical Methods in Fluids*, **31**, pp. 431–449.

[20] Issa, R. I., 1986. "Solution of the Implicitly Discretised Fluid flow Equations by Operator-Splitting". *Journal of Computational Physics*, **62**, pp. 40–65.

[21] Dellenback, P. A., Metzger, D. E., and p. Neitzel, 1988. "Measurements in Turbulent Swirling Flow through an Abrupt Axisymmetric Expansion". *AIAA.J.*, **26**(6), pp. 669–681.